Supplementary Figures

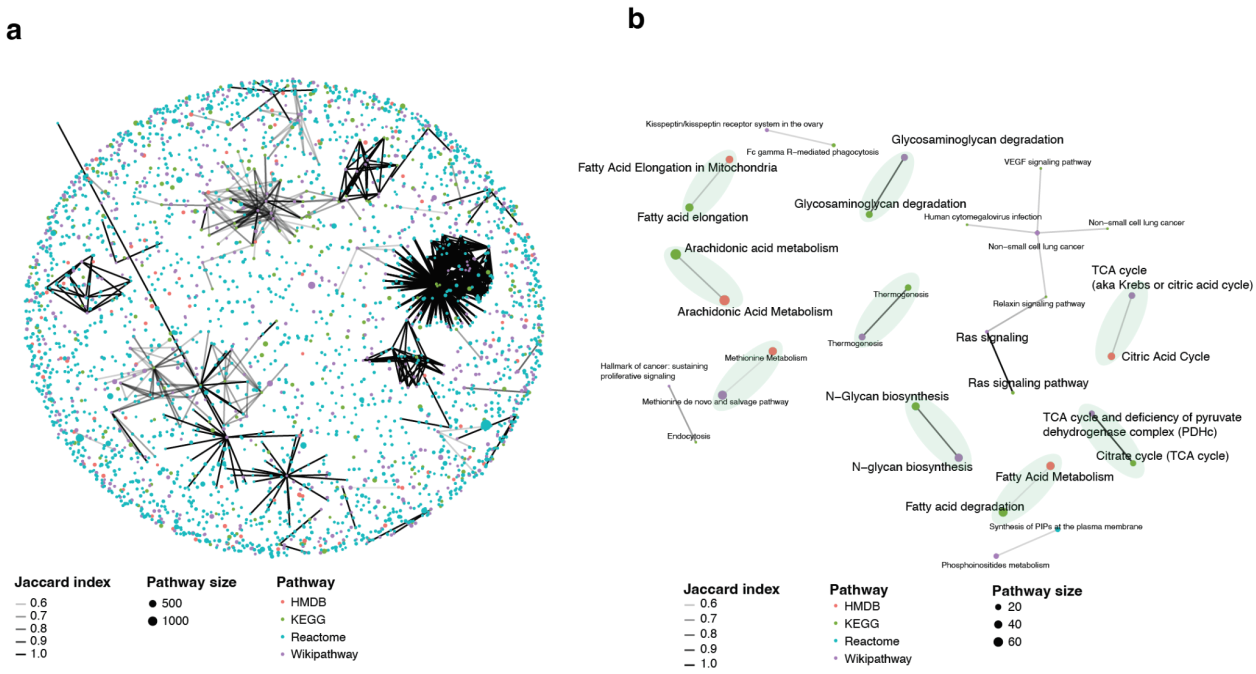

Supplementary Figure 1 | Similarity network of metabolic pathways across four public databases. a, Global network visualization of metabolic pathways from HMDB, KEGG, Reactome, and WikiPathways. Nodes represent individual pathways, colored by their database of origin. Edges denote pairwise similarity based on the Jaccard index, with edge thickness indicating the degree of overlap. Node size reflects the number of metabolites within each pathway. **b,** Enlarged subnetwork highlighting clusters of highly similar or identical pathways shared across multiple databases. These clusters illustrate redundancy and overlap in pathway definitions, underscoring the need for integrated pathway analysis in untargeted metabolomics.

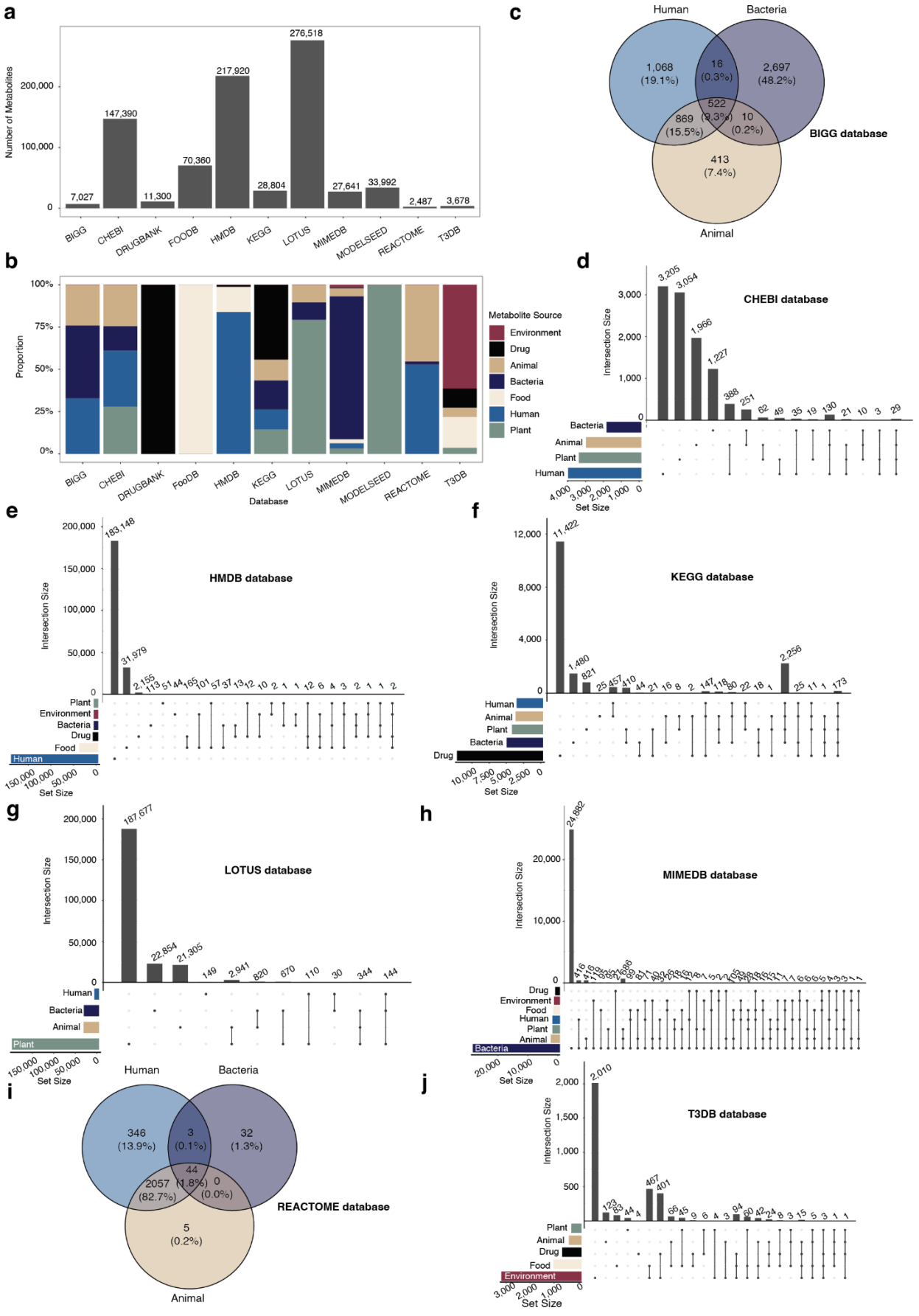
a
Number of Metabolites
200,000
100,000
0
7,027
147,390
11,300
70,360
217,920
28,804
276,518
27,641
33,992
2,487
3,678
BIGG
CHEBI
DRUGBANK
FOODB
HMDB
KEGG
LOTUS
MIMEDB
MODELSEED
REACTOME
T3DB
b
Proportion
100%
75%
50%
25%
0%
Database
Metabolite Source
Environment
Drug
Animal
Bacteria
Food
Human
Plant
c
Human
Bacteria
1,068
(19.1%)
16
(0.3%)
2,697
(48.2%)
522
(9.3%)
869
(15.5%)
10
(0.2%)
BIGG database
413
(7.4%)
Animal
d
CHEBI database
Intersection Size
3,205
3,054
1,966
1,227
388
251
62
49
35
19
130
21
10
3
29
Bacteria
Animal
Plant
Human
Set Size
e
HMDB database
Intersection Size
183,148
31,979
2,155
113
51
44
165
101
57
37
13
12
10
2
1
1
12
6
4
3
2
1
1
2
Plant
Environment
Bacteria
Drug
Food
Human
Set Size
f
KEGG database
Intersection Size
11,422
1,480
821
25
457
410
44
21
16
8
2
147
118
80
22
18
1
2,256
25
11
1
173
Human
Animal
Plant
Bacteria
Drug
Set Size
g
LOTUS database
Intersection Size
187,677
22,854
21,305
149
2,941
820
670
110
30
344
144
Human
Bacteria
Animal
Plant
Set Size
h
MIMEDB database
Intersection Size
24,882
Drug
Environment
Food
Human
Plant
Animal
Bacteria
Set Size
i
Human
Bacteria
346
(13.9%)
3
(0.1%)
32
(1.3%)
44
(1.8%)
2057
(82.7%)
0
(0.0%)
REACTOME database
5
(0.2%)
Animal
j
T3DB database
Intersection Size
2,010
123
83
44
467
401
66
45
9
6
4
3
94
60
42
24
8
3
15
5
3
1
1
Plant
Animal
Drug
Food
Environment
Set Size

Supplementary Figure 2 | Detailed overview of the integrated metabolite database with source information. a, Number of metabolites contributed by each of the 11 integrated public databases. **b,** Proportional distribution of source categories (human, animal, bacteria, plant, food, drug, and environment) within each database. **c-j,** Source overlap analysis across individual databases. **c,** The Venn diagram shows the source category overlap in the BiGG database. **d-f,** UpSet plots illustrating source intersections for metabolites in the ChEBI **(d)**, HMDB **(e)**, and KEGG **(f)** databases. **g-h,** UpSet plots showing source distribution in the LOTUS **(g)** and MiMeDB **(h)** databases. **i,** Venn diagram of source category overlap for the Reactome database. **j,** UpSet plot for source classification in the T3DB database.

a

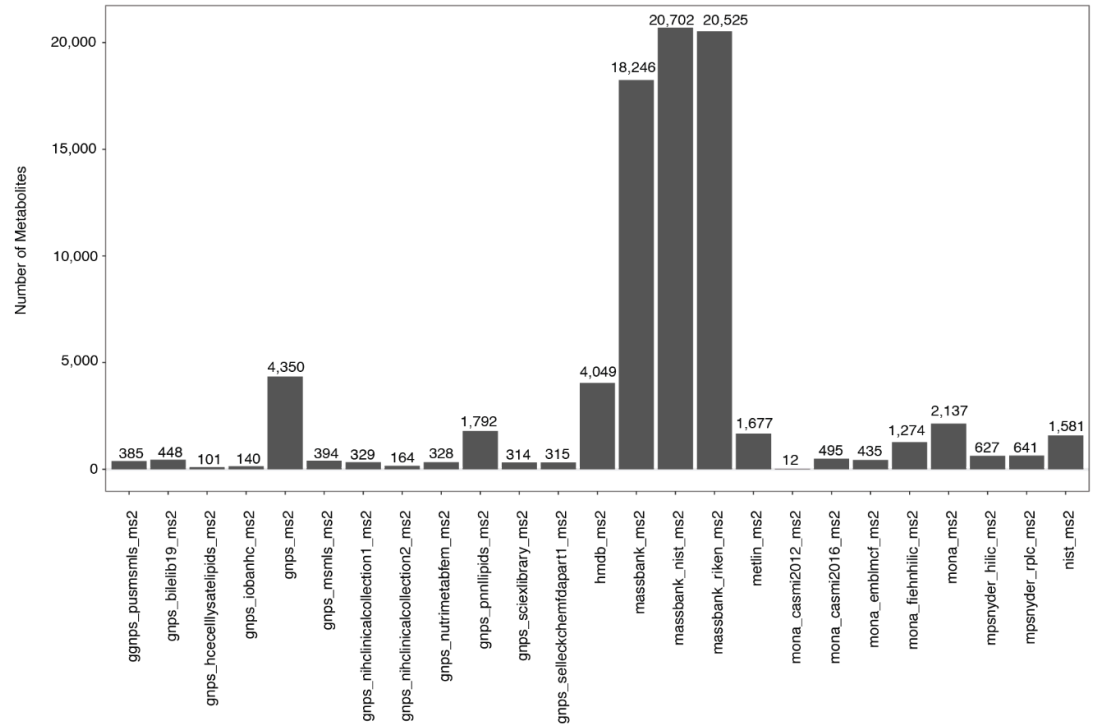
Number of Metabolites
20,000
15,000
10,000
5,000
0
385
448
101
140
4,350
394
329
164
328
1,792
314
315
4,049
18,246
20,702
20,525
1,677
12
495
435
1,274
2,137
627
641
1,581
ggnps_pusmsmls_ms2
gnps_bilelib19_ms2
gnps_hcecellsatelipids_ms2
gnps_iobanhc_ms2
gnps_ms2
gnps_msmls_ms2
gnps_nihclinicalcollection1_ms2
gnps_nihclinicalcollection2_ms2
gnps_nutrimetabfem_ms2
gnps_pnnllipids_ms2
gnps_sciexlibrary_ms2
gnps_selleckchemfdapart1_ms2
hmdb_ms2
massbank_ms2
massbank_nist_ms2
massbank_riken_ms2
metlin_ms2
mona_casmi2012_ms2
mona_casmi2016_ms2
mona_emblmcf_ms2
mona_fiehnhilic_ms2
mona_ms2
mpsnyder_hilic_ms2
mpsnyder_rplc_ms2
nist_ms2

b

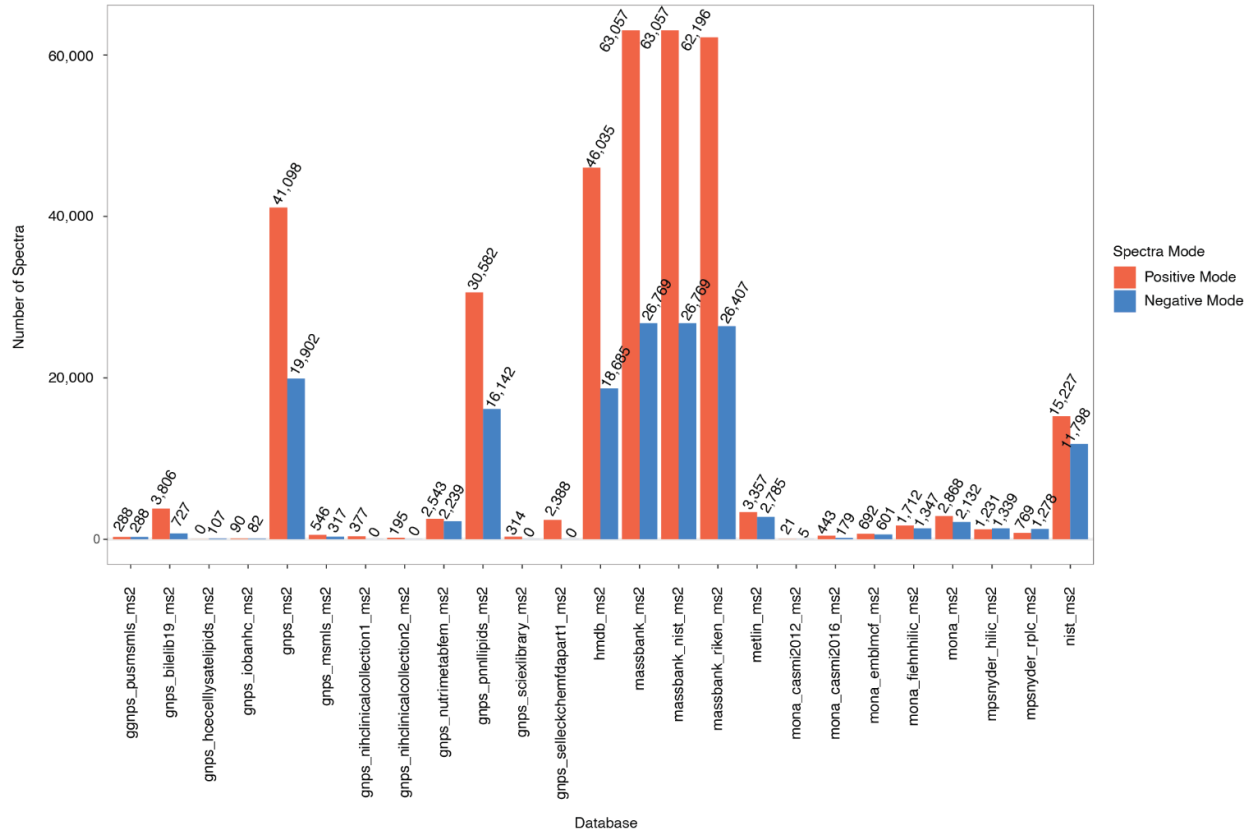
Number of Spectra
60,000
40,000
20,000
0
288
288
3,806
727
0
107
90
82
41,098
19,902
546
317
377
0
195
0
2,543
2,239
30,582
16,142
314
0
2,388
0
46,035
18,685
63,057
26,769
63,057
26,769
62,196
26,407
3,357
2,785
21
5
443
179
692
601
1,712
1,347
2,868
2,132
1,231
1,339
769
1,278
15,227
11,798
ggnps_pusmsmls_ms2
gnps_bilelib19_ms2
gnps_hcecellsatelipids_ms2
gnps_iobanhc_ms2
gnps_ms2
gnps_msmls_ms2
gnps_nihclinicalcollection1_ms2
gnps_nihclinicalcollection2_ms2
gnps_nutrimetabfem_ms2
gnps_pnnllipids_ms2
gnps_sciexlibrary_ms2
gnps_selleckchemfdapart1_ms2
hmdb_ms2
massbank_ms2
massbank_nist_ms2
massbank_riken_ms2
metlin_ms2
mona_casmi2012_ms2
mona_casmi2016_ms2
mona_emblmcf_ms2
mona_fiehnhilic_ms2
mona_ms2
mpsnyder_hilic_ms2
mpsnyder_rplc_ms2
nist_ms2
Database
Spectra Mode
Positive Mode
Negative Mode

Supplementary Figure 3 | Overview of the merged MS^2 spectral database integrated in TidyMass2. a, Total number of unique metabolites represented across 25 public and in-house MS^2 spectral databases. **b,** Distribution of MS^2 spectra across positive and negative ionization modes for each database.

a

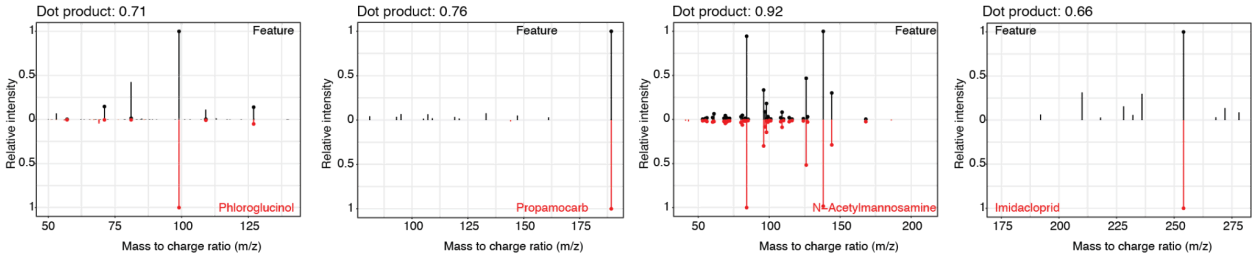

Supplementary Figure 4 | Validation of level 2 annotations by MS^2 spectra of standard compounds. a, Comparison of MS^2 spectra with the standard compounds for the 4 annotated features.

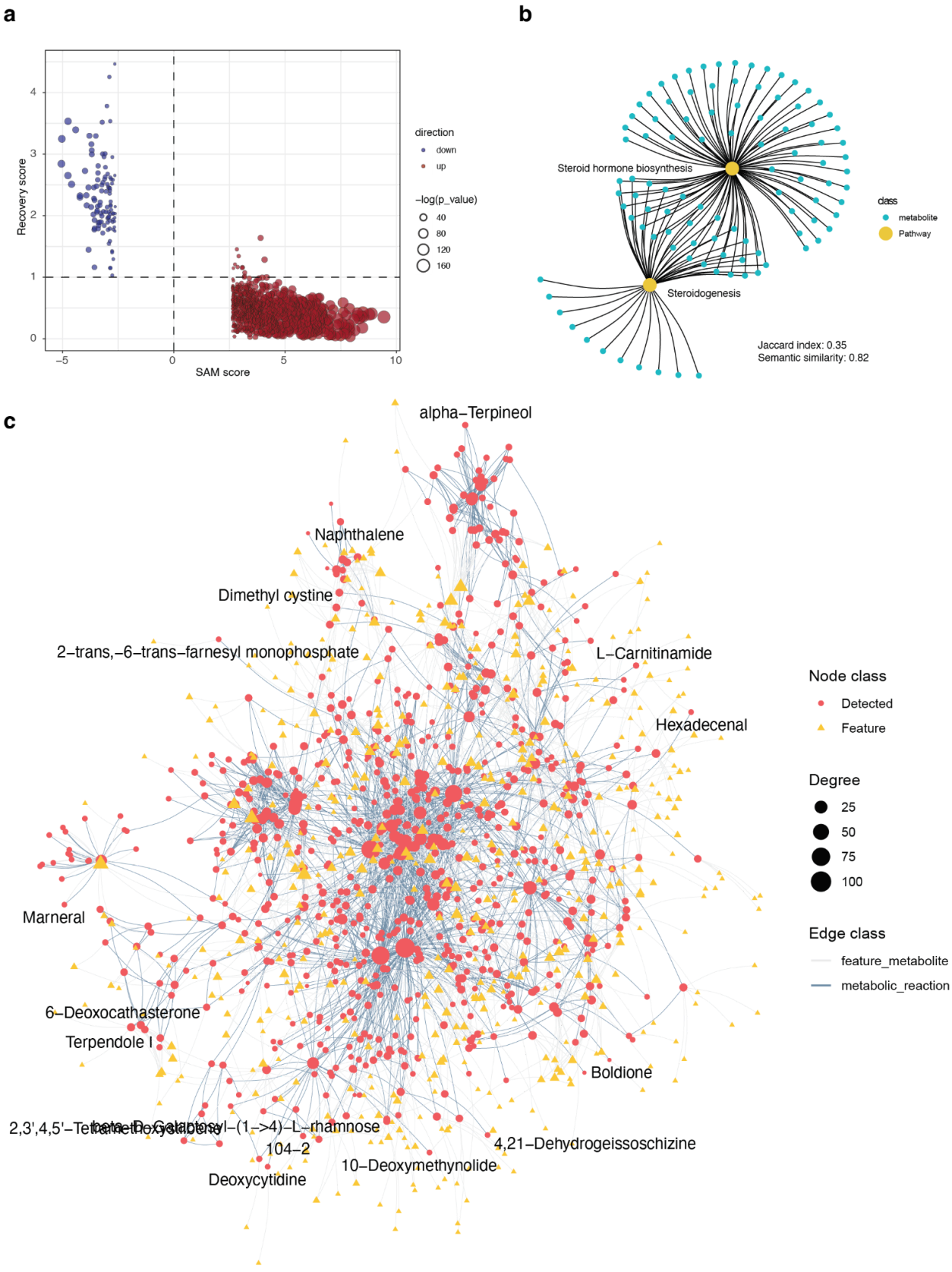
a
Recovery score
SAM score
direction
down
up
−log(p_value)
40
80
120
160
b
Steroid hormone biosynthesis
Steroidogenesis
class
metabolite
Pathway
Jaccard index: 0.35
Semantic similarity: 0.82
c
alpha−Terpineol
Naphthalene
Dimethyl cystine
2−trans,−6−trans−farnesyl monophosphate
L−Carnitinamide
Hexadecenal
Marneral
6−Deoxocathasterone
Terpendole I
Boldione
2,3',4,5'−Tetramethoxystilbene
beta−D−Galactosyl−(1−>4)−L−rhamnose
104−2
Deoxycytidine
10−Deoxymethynolide
4,21−Dehydrogeissoschizine
Node class
Detected
Feature
Degree
25
50
75
100
Edge class
feature_metabolite
metabolic_reaction

Supplementary Figure 5 | Dysregulated metabolic features and network remodeling during pregnancy. a, Scatter plot showing SAM scores and recovery scores for all significantly dysregulated metabolic features across pregnancy. A positive SAM score indicates increased abundance during pregnancy, while a negative SAM score indicates decreased levels. Recovery scores reflect post-delivery changes relative to late pregnancy: scores < 0 suggest postpartum decline, and scores >0 indicate postpartum elevation. **b,** Network visualization showing the overlap between two pathways from different databases, demonstrating pathway convergence across sources. **c,** Global dysregulated metabolic network identified using the metabolic feature-based module analysis in TidyMass2. Nodes represent either metabolic features (yellow triangles) or putatively annotated metabolites (red circles), with node size reflecting connectivity (degree). Edges denote biological relationships based on reaction pairs or metabolite-feature annotations.

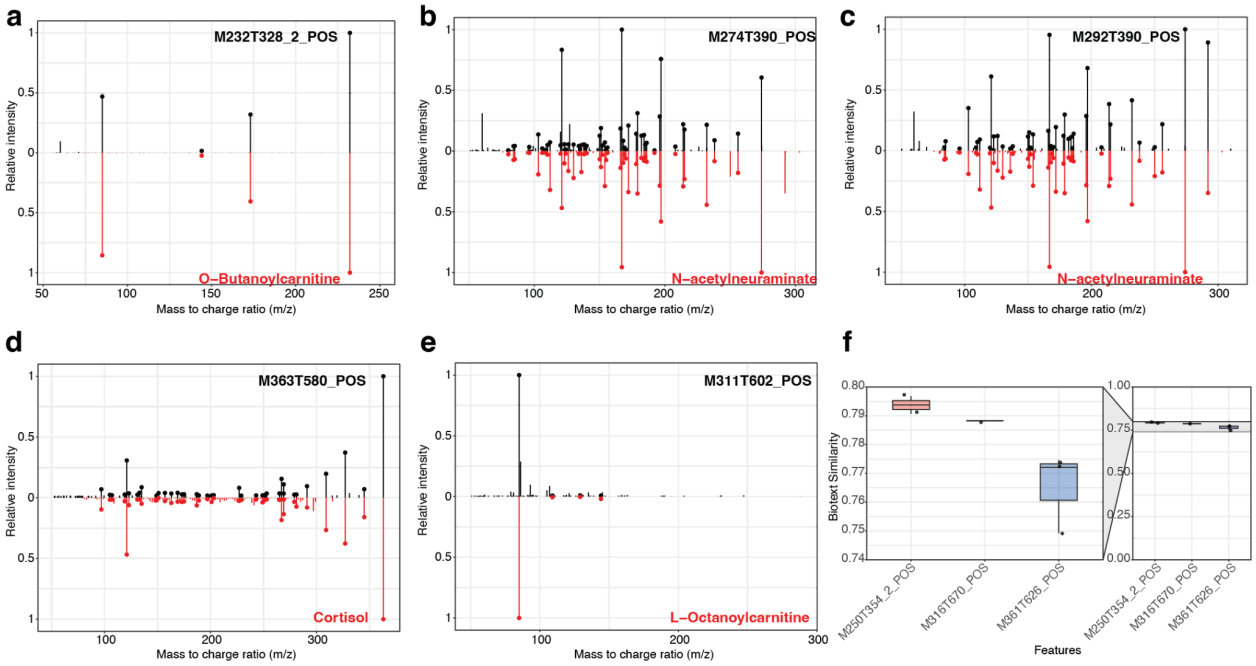

Supplementary Figure 6 | Validation of FFMA-annotated features using in-house library and biological similarity analysis. a-e, Comparison of MS^2 spectra with the library for the 5 matched features: **a,** M232T328_2_POS; **b,** M274T390_POS; **c,** M292T390_POS; **d,** M363T580_POS; **e,** M311T602_POS. **f,** Biological similarity between the FFMA annotations and the true annotations for the 3 unmatched features.

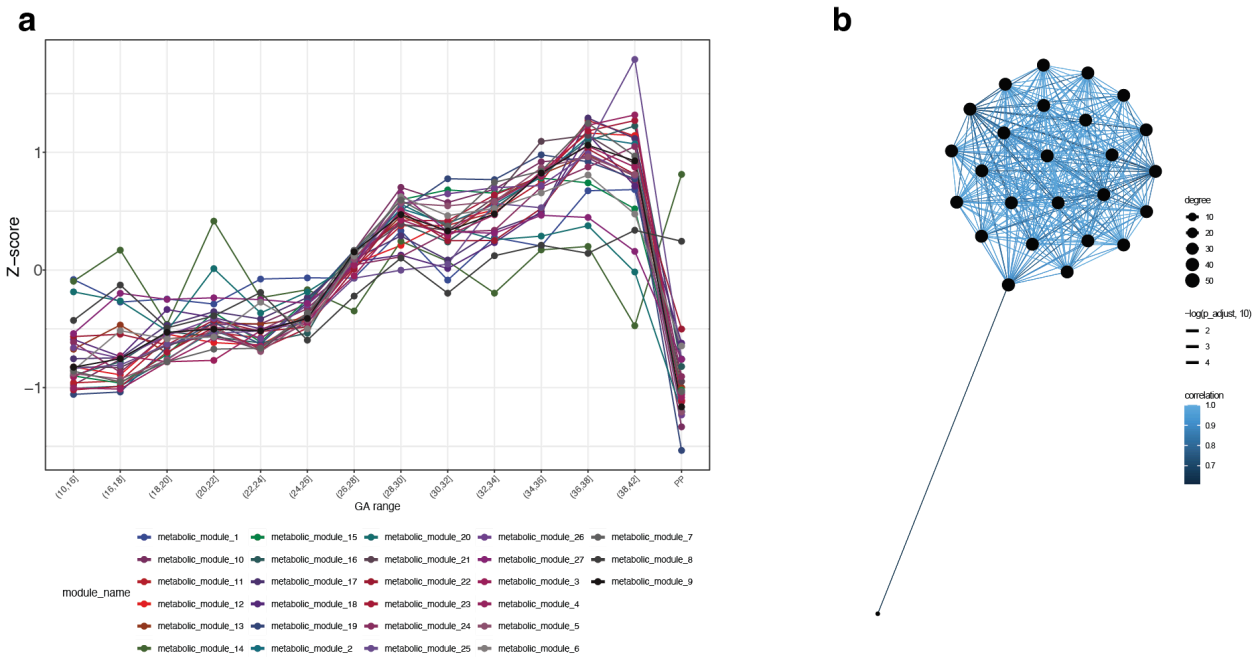

Supplementary Figure 7 | Temporal dynamics and interconnectivity of dysregulated metabolic modules during pregnancy. a, Line plot showing longitudinal changes in the abundance of 27 dysregulated metabolic modules across gestation. Each line represents the Z-score trajectory of a single module across gestational age (GA) intervals, with a sharp decline observed postpartum (PP). **b,** Correlation network illustrating relationships among the 27 metabolic modules. Node size indicates degree (number of connections), edge width reflects the significance of correlations (adjusted p-value), and edge color denotes the strength of correlations. This network highlights coordinated metabolic remodeling during pregnancy.

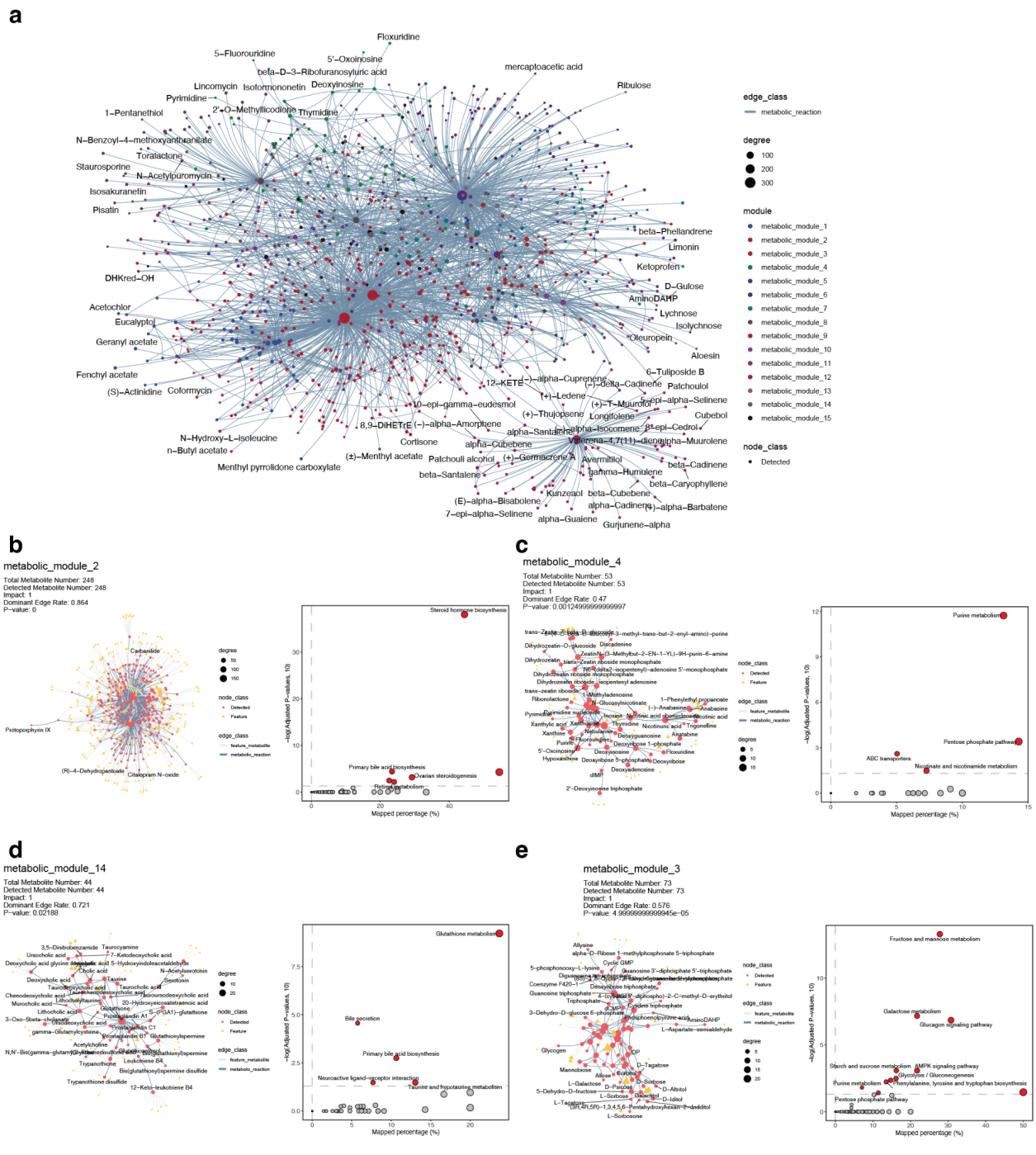

Supplementary Figure 8 | Dysregulated metabolic modules identified in blood samples from CIDP patients using feature-based functional module analysis. a, Network visualization of the 15 dysregulated metabolic modules identified using TidyMass2's feature-based functional module analysis. **b,** Metabolic module 2 is associated with steroid hormone metabolism. **c,** Metabolic module 4 is associated with purine metabolism. **d,** Metabolic module 14 represents bile acid metabolism. **e,** Metabolic module 3 corresponds to carbohydrate and energy

metabolism. Pathway enrichment analysis was performed using a one-sided hypergeometric test and *p-values* were adjusted for multiple comparisons using the Benjamini-Hochberg (BH) method. Metabolic module significance was assessed using a one-sided permutation-based test with a Gamma-fitted null distribution; no additional multiple-comparison correction was applied at the module level.

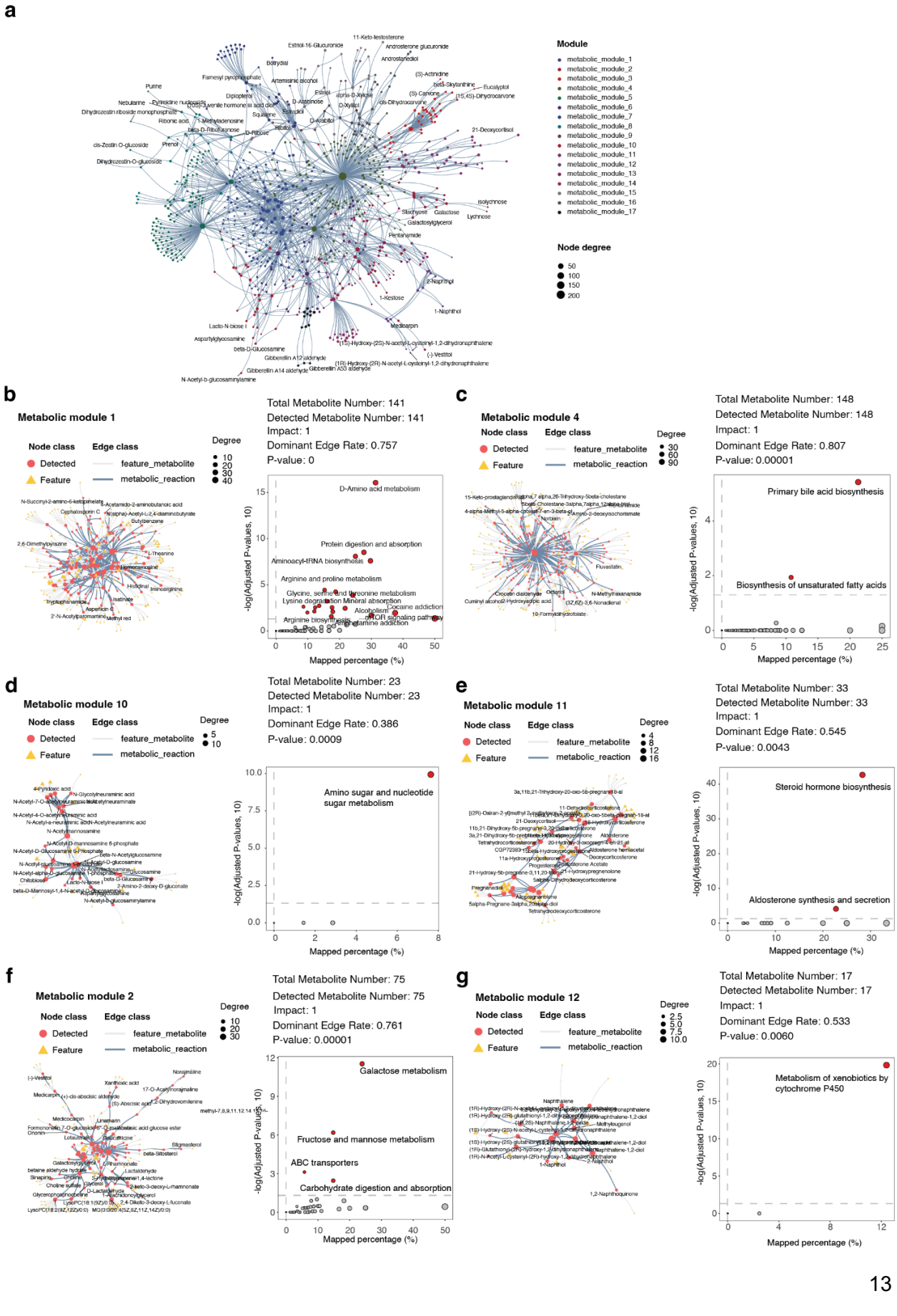
a
Module
metabolic_module_1
metabolic_module_2
metabolic_module_3
metabolic_module_4
metabolic_module_5
metabolic_module_6
metabolic_module_7
metabolic_module_8
metabolic_module_9
metabolic_module_10
metabolic_module_11
metabolic_module_12
metabolic_module_13
metabolic_module_14
metabolic_module_15
metabolic_module_16
metabolic_module_17
Node degree
50
100
150
200
b
Metabolic module 1
Node class
Detected
Feature
Edge class
feature_metabolite
metabolic_reaction
Degree
10
20
30
40
Total Metabolite Number: 141
Detected Metabolite Number: 141
Impact: 1
Dominant Edge Rate: 0.757
P-value: 0
D-Amino acid metabolism
Protein digestion and absorption
Aminoacyl-tRNA biosynthesis
Arginine and proline metabolism
Glycine, serine and threonine metabolism
Lysine degradation
Mineral absorption
Alcoholism
Cocaine addiction
Arginine biosynthesis
mTOR signaling pathway
Amphetamine addiction
-log(Adjusted P-values, 10)
Mapped percentage (%)
c
Metabolic module 4
Node class
Detected
Feature
Edge class
feature_metabolite
metabolic_reaction
Degree
30
60
90
Total Metabolite Number: 148
Detected Metabolite Number: 148
Impact: 1
Dominant Edge Rate: 0.807
P-value: 0.00001
Primary bile acid biosynthesis
Biosynthesis of unsaturated fatty acids
-log(Adjusted P-values, 10)
Mapped percentage (%)
d
Metabolic module 10
Node class
Detected
Feature
Edge class
feature_metabolite
metabolic_reaction
Degree
5
10
Total Metabolite Number: 23
Detected Metabolite Number: 23
Impact: 1
Dominant Edge Rate: 0.386
P-value: 0.0009
Amino sugar and nucleotide sugar metabolism
-log(Adjusted P-values, 10)
Mapped percentage (%)
e
Metabolic module 11
Node class
Detected
Feature
Edge class
feature_metabolite
metabolic_reaction
Degree
4
8
12
16
Total Metabolite Number: 33
Detected Metabolite Number: 33
Impact: 1
Dominant Edge Rate: 0.545
P-value: 0.0043
Steroid hormone biosynthesis
Aldosterone synthesis and secretion
-log(Adjusted P-values, 10)
Mapped percentage (%)
f
Metabolic module 2
Node class
Detected
Feature
Edge class
feature_metabolite
metabolic_reaction
Degree
10
20
30
Total Metabolite Number: 75
Detected Metabolite Number: 75
Impact: 1
Dominant Edge Rate: 0.761
P-value: 0.00001
Galactose metabolism
Fructose and mannose metabolism
ABC transporters
Carbohydrate digestion and absorption
-log(Adjusted P-values, 10)
Mapped percentage (%)
g
Metabolic module 12
Node class
Detected
Feature
Edge class
feature_metabolite
metabolic_reaction
Degree
2.5
5.0
7.5
10.0
Total Metabolite Number: 17
Detected Metabolite Number: 17
Impact: 1
Dominant Edge Rate: 0.533
P-value: 0.0060
Metabolism of xenobiotics by cytochrome P450
-log(Adjusted P-values, 10)
Mapped percentage (%)

Supplementary Figure 9 | Dysregulated metabolic modules identified in blood samples during pregnancy using feature-based functional module analysis. a, Network visualization of the 17 dysregulated metabolic modules identified using TidyMass2's feature-based module. **b,** Metabolic module 1 is associated with amino acid metabolism. **c,** Metabolic module 4 representing lipid metabolism. **d,** Metabolic module 10 representing amino sugar and nucleotide sugar metabolism. **e,** Metabolic module 11 is associated with steroid hormone metabolism. **f,** Metabolic module 2 is associated with carbohydrate transport and utilization. **g,** Metabolic module 12 representing xenobiotic metabolism by cytochrome P450. Pathway enrichment analysis was performed using a one-sided hypergeometric test and *p-values* were adjusted for multiple comparisons using the Benjamini-Hochberg (BH) method. Metabolic module significance was assessed using a one-sided permutation-based test with a Gamma-fitted null distribution; no additional multiple-comparison correction was applied at the module level.

Supplementary Tables

Supplementary Table 1. Databases used in TidyMass2

Database	Link	Metabolite source information	MS^2 spectra	Pathway	Chemical reaction
KEGG	https://www.genome.jp/kegg/	Yes	No	Yes	Yes
HMDB	https://www.hmdb.ca/	Yes	Yes	Yes	Yes
Reactome	https://reactome.org/	Yes	No	Yes	Yes
BIGG	http://bigg.ucsd.edu/	Yes	No	No	Yes
CHEBI	https://www.ebi.ac.uk/chebi/	Yes	No	No	No
DrugBank	https://go.drugbank.com/	Yes	No	No	No
FooDB	https://foodb.ca/	Yes	No	No	No
Lotus	https://lotus.naturalproducts.net/	Yes	No	No	No
MIMEDB	https://mimedb.org/	Yes	No	No	No
Modelseed	https://modelseed.org/	Yes	No	No	Yes
T3DB	https://www.t3db.ca/	Yes	No	No	No
WikiPathways	https://www.wikipathways.org/	No	No	Yes	No
SMPDB	https://smpdb.ca/	No	No	Yes	No
LipidBank	https://lipidbank.jp/	No	No	No	No

LipidMaps	https://www.lipidmaps.org/	No	No	No	No
WikiPedia	https://www.wikipedia.org/	No	No	No	No
GNPS	https://gnps.ucsd.edu/ProteoSAFe/static/gnps-splash.jsp?redirect=auth	No	Yes	No	No
MassBank	https://massbank.eu/MassBank/	No	Yes	No	No
Mona	https://mona.fiehnlab.ucdavis.edu/	No	Yes	No	No
Recon3	https://www.vmh.life/	No	No	No	Yes
MetaNetx	https://www.metanetx.org/	No	No	No	Yes
Rhea	https://www.rhea-db.org/	No	No	No	Yes

Supplementary Table 2. Comparison between TidyMass2 and existing tools.

Name	TidyMass2	RforMassSpectrometry	MetaboAnalyst	MetOrigin2	MicrobeMASST	PIUMet	Mummichog	MSDIAL
Comprehensive and integrated workflow	+++	++	+++	+	+	+	+	++
Command-line interface	✓	✓	✓	-	✓	-	✓	-
GUI/Online interface	✓	-	✓	✓	✓	✓	✓	✓
Cross-platform utility	+++	+++	+++	+++	+++	+++	+++	+
Local PC deployment	✓	✓	✓	-	-	-	✓	✓
Server deployment	✓	✓	✓	-	-	-	✓	-
Customized metabolite database	✓	-	-	-	-	-	-	✓
Customized pathway database	✓	-	-	-	-	-	-	-
Feature-based module analysis	✓	-	✓	-	-	✓	✓	-
Metabolite origin analysis	✓	-	-	✓	✓	✓	-	-
Open-source (code)	+++	+++	+++	-	+	-	+++	+++
Open-source (databases)	+++	-	-	-	+++	+	-	+++

Note: Symbols used for feature evaluations with "√" for present, "-" for absent, and "+" for a more quantitative assessment, with more "+" indicating better support.

Supplementary Table 3. 27 dysregulated metabolic modules.

Name	P value	Metabolite number	Metabolite ID (KEGG)
metabolic_module_1	0	41	C06099{}C00521{}C11398{}C11412{}C01123{}C01765{}C07271{}C11393{}C11399{}C11410{}C11411{}C11416{}C11384{}C00964{}C02452{}C09902{}C20261{}C02344{}C01766{}C09847{}C11408{}C11396{}C11395{}C11409{}C11397{}C11400{}C11413{}C11401{}C11418{}C11415{}C16462{}C16461{}C11924{}C01499{}C09848{}C02576{}C11383{}C01767{}C11338{}C11420{}C20260
metabolic_module_2	0	84	C00763{}C01905{}C00079{}C00041{}C00148{}C00152{}C00407{}C00135{}C00047{}C00065{}C00062{}C00123{}C00183{}C00078{}C00077{}C00792{}C01682{}C00064{}C00097{}C02486{}C00303{}C03793{}C05552{}C07541{}C06735{}C16438{}C16590{}C16593{}C03912{}C03564{}C19716{}C20277{}C20278{}C20313{}C17349{}C20978{}C22162{}C02356{}C00334{}C03406{}C15767{}C02155{}C03227{}C02794{}C01165{}C01157{}C00884{}C06121{}C02265{}C05933{}C04020{}C21015{}C11332{}C02993{}C16435{}C01015{}C05147{}C05636{}C07544{}C08290{}C16696{}C16831{}C17255{}C19706{}C19781{}C20330{}C20487{}C20488{}C20802{}C20850{}C21026{}C21092{}C21160{}C21283{}C04322{}C01924{}C02427{}C02728{}C01877{}C04148{}C02710{}C01570{}C03230{}C00977
metabolic_module_3	0	28	C00185{}C00031{}C00116{}C00267{}C00897{}C00208{}C01083{}C00103{}C01971{}C06421{}C02048{}C02074{}C02655{}C03855{}C08240{}C11546{}C15548{}C15970{}C00252{}C00221{}C01518{}C01594{}C08334{}C13857{}C04197{}C19636{}C02130{}C08325
metabolic_module_4	0	109	C00019{}C01917{}C00021{}C07349{}C02890{}C00580{}C00409{}C05204{}C06347{}C06629{}C07028{}C07966{}C03114{}C21584{}C09390{}C11839{}C11840{}C12044{}C12416{}C12476{}C05315{}C15682{}C15681{}C02483{}C20248{}C16230{}C16708{}C16713{}C16789{}C17702{}C17703{}C20444{}C20629{}C20673{}C20677{}C20819{}C21183{}C21198{}C21201{}C21281{}C21427{}C21428{}C21429{}C21433{}C21434{}C21436{}C21647{}C21648{}C22142{}C05298{}C00978{}C00189{}C00780{}C01161{}C16675{}C07481{}C13747{}C07130{}C07480{}C14152{}C00346{}C00588{}C13482{}C00385{}C02666{}C02918{}C01586{}C20674{}C02442{}C06212{}C09642{}C00758{}C00841{}C08608{}C21602{}C01957{}C05203{}C08299{}C05831{}C05902{}C01008{}C05594{}C08526{}C02079{}C02381{}C04208{}C04444{}C08263{}C10159{}C15530{}C15536{}C15616{}C15883{}C16419{}C19895{}C20234{}C20790{}C20872{}C01004{}C10652{}C06199{}C05317{}C06812{}C04293{}C08304{}C15531{}C10098{}C19807{}C03986

metabolic_module_5	2.00E-05	77	C00020{}C00314{}C00133{}C00740{}C00022{}C00515{}C02713{}C00246{}C02703{}C00109{}C00163{}C00466{}C03943{}C03341{}C03248{}C04137{}C00956{}C05556{}C09822{}C00164{}C00627{}C01089{}C12477{}C12986{}C16138{}C16149{}C00441{}C02291{}C17237{}C19694{}C19719{}C02218{}C03283{}C05984{}C00542{}C02488{}C00250{}C01077{}C21096{}C01712{}C01607{}C01588{}C03401{}C08316{}C06429{}C08323{}C08367{}C16525{}C16536{}C03197{}C01118{}C01401{}C00534{}C08739{}C05714{}C16434{}C04210{}C02721{}C04076{}C03210{}C00736{}C00450{}C01275{}C16436{}C01136{}C01110{}C01092{}C00793{}C01037{}C03340{}C02132{}C02527{}C20258{}C20904{}C22087{}C03996{}C00716
metabolic_module_6	1.00E-04	25	C00794{}C00089{}C02209{}C00159{}C00095{}C00392{}C00668{}C01096{}C00085{}C00636{}C00092{}C01172{}C17209{}C04006{}C20236{}C20861{}C00275{}C00644{}C01742{}C03267{}C06468{}C06187{}C06019{}C19761{}C20887
metabolic_module_7	0.00023	34	C01732{}C00042{}C03325{}C01851{}C02046{}C06658{}C06659{}C06660{}C10842{}C11860{}C11857{}C11862{}C11859{}C11863{}C11866{}C11868{}C06094{}C15770{}C18312{}C11864{}C03648{}C11858{}C03761{}C00490{}C00859{}C06095{}C11865{}C02034{}C14162{}C02035{}C06096{}C11869{}C20632{}C11855
metabolic_module_8	0.00046	21	C01697{}C00243{}C01970{}C00764{}C00984{}C00124{}C05402{}C05401{}C01113{}C00962{}C01097{}C00795{}C01235{}C05399{}C05400{}C03384{}C01582{}C04452{}C21523{}C21524{}C02965
metabolic_module_9	0.00053	33	C00427{}C00219{}C11878{}C11881{}C18220{}C18222{}C06428{}C11887{}C14770{}C18211{}C18219{}C18221{}C11882{}C06425{}C16527{}C03242{}C14771{}C00909{}C05956{}C13856{}C14768{}C14769{}C14748{}C20388{}C18177{}C12083{}C14822{}C12077{}C09118{}C20329{}C14807{}C14778{}C14749
metabolic_module_10	0.00077	20	C00270{}C00140{}C03878{}C00329{}C08349{}C04501{}C00357{}C01674{}C00611{}C19910{}C19909{}C04017{}C04015{}C04256{}C00645{}C06372{}C04257{}C01075{}C04016{}C04886
metabolic_module_11	0.00224	35	C00712{}C00487{}C15025{}C00318{}C02290{}C00823{}C04114{}C01181{}C06424{}C06427{}C21761{}C00249{}C01530{}C08320{}C06426{}C16300{}C16522{}C02862{}C19670{}C06123{}C00517{}C05828{}C01149{}C01259{}C01948{}C08388{}C02571{}C19936{}C20704{}C22135{}C20826{}C02838{}C03017{}C03195{}C17535
metabolic_module_12	0.00389	17	C15788{}C15787{}C15789{}C15790{}C15791{}C15799{}C15798{}C15797{}C15800{}C16253{}C15792{}C16251{}C15801{}C15793{}C17733{}C15786{}C17735
metabolic_module_13	0.00924	23	C06069{}C01500{}C06070{}C11389{}C11404{}C11402{}C17622{}C20222{}C20223{}C10469{}C10453{}C17621{}C03985{}C04433{}C09861{}C01433{}C06071{}C10428{}C09987{}C20221{}C20225{}C10478{}C09910
metabolic_module	0.01093	12	C14786{}C04314{}C00829{}C14787{}C11714{}C11713{}C06205{}C14791{}C14793{}C14792{}C04514{}C

_14			14784
metabolic_module_15	0.01174	10	C21030{}C01188{}C06002{}C18318{}C02170{}C06001{}C03284{}C01205{}C00349{}C20846
metabolic_module_16	0.01175	28	C00881{}C01121{}C11992{}C03240{}C06630{}C06616{}C00363{}C11955{}C11963{}C11972{}C11991{}C11993{}C11997{}C12000{}C12002{}C12384{}C12385{}C12404{}C12407{}C12412{}C12424{}C12472{}C12481{}C18034{}C18635{}C18634{}C06635{}C21350
metabolic_module_17	0.01764	14	C00280{}C00674{}C00523{}C07632{}C01227{}C03772{}C04295{}C05139{}C05290{}C05140{}C20144{}C11135{}C20252{}C18045
metabolic_module_18	0.02119	11	C19756{}C19743{}C01126{}C19746{}C09704{}C03220{}C20325{}C16537{}C03461{}C19691{}C20121
metabolic_module_19	0.02135	11	C03375{}C00750{}C00986{}C02567{}C01029{}C00612{}C05665{}C03413{}C05936{}C02946{}C18170
metabolic_module_20	0.02455	8	C00546{}C00583{}C00424{}C05235{}C00937{}C02912{}C02917{}C15499
metabolic_module_21	0.02522	13	C05487{}C00735{}C18075{}C05488{}C05138{}C02373{}C05501{}C05499{}C05284{}C02821{}C14256{}C05489{}C02822
metabolic_module_22	0.02527	24	C00132{}C01761{}C02151{}C03677{}C05616{}C09694{}C11632{}C11633{}C11807{}C16502{}C16503{}C16504{}C16505{}C18640{}C06800{}C19613{}C11045{}C13244{}C03686{}C17530{}C16508{}C16506{}C16507{}C19681
metabolic_module_23	0.03215	19	C00235{}C06067{}C09023{}C20512{}C20532{}C20543{}C20545{}C20563{}C20982{}C20983{}C18083{}C04290{}C02008{}C06068{}C18053{}C19767{}C20594{}C20636{}C16521
metabolic_module_24	0.0364	26	C01054{}C08624{}C11505{}C01902{}C01724{}C11455{}C08628{}C17966{}C19820{}C19832{}C19833{}C20187{}C20188{}C20189{}C20191{}C20192{}C20193{}C20194{}C20195{}C20200{}C19835{}C08637{}C19918{}C19801{}C08615{}C08626
metabolic_module_25	0.03701	6	C00101{}C00143{}C21801{}C21802{}C00664{}C00445
metabolic_module_26	0.03713	18	C08062{}C00108{}C00196{}C00885{}C00251{}C00805{}C10733{}C00134{}C20579{}C00254{}C21147{}C03005{}C00555{}C15668{}C00826{}C10497{}C01405{}C03002
metabolic_module	0.04192	10	C02991{}C01934{}C19758{}C02338{}C02476{}C00507{}C02431{}C20354{}C03979{}C00861

_27			

Note: Metabolic module significance was assessed using a one-sided permutation-based test with a Gamma-fitted null distribution; no additional multiple-comparison correction was applied.

Supplementary Table 4. Identified pathways for dysregulated metabolic modules.

Pathway ID	Pathway name	p_value_adjust	Metabolite ID (KEGG)
hsa00330	Arginine and proline metabolism	1.97E-11	C03912;C00986;C03564;C15767;C02946;C00334;C00555;C01877;C01110;C04137;C00763;C10497;C00884;C01157;C00062;C00441;C01165;C00077;C00148;C05933;C05936;C01682;C03375;C00134;C00022;C00019;C00750;C19706;C05147
hsa00052	Galactose metabolism	1.73E-10	C05401;C00095;C00085;C00124;C01113;C00031;C00103;C00159;C00794;C00795;C01097;C05400;C01697;C00116;C00243;C05399;C05402;C00089;C00984;C01235;C00267;C00668
hsa05230	Central carbon metabolism in cancer	9.85E-09	C00085;C00031;C00092;C00041;C00062;C00152;C00097;C00064;C00135;C00407;C00123;C00079;C00148;C00065;C00078;C00183;C00022;C00042
hsa00470	D-Amino acid metabolism	1.49E-08	C03943;C03564;C03341;C01110;C00133;C00792;C00793;C00515;C02265;C00763;C00740;C01157;C00041;C00062;C00097;C00064;C00135;C00047;C00077;C00079;C00148;C00065;C00134;C00022
hsa02010	ABC transporters	2.30E-07	C04114;C01181;C00487;C00185;C01674;C00095;C00031;C00159;C04137;C00794;C00881;C00116;C01157;C00041;C00062;C00064;C00135;C00407;C00123;C00047;C00077;C00079;C00148;C00065;C00183;C00243;C00208;C00392;C05402;C00140;C01682;C00134;C00089;C01083
hsa04974	Protein digestion and absorption	5.83E-07	C00246;C00041;C00062;C00152;C00097;C00064;C00135;C00407;C00123;C00047;C00079;C00148;C16138;C00065;C00078;C00183;C00163;C00134
hsa00051	Fructose and mannose metabolism	3.48E-05	C00424;C03979;C00095;C00644;C00159;C00636;C00275;C00794;C02431;C01934;C02991;C00507;C00861;C00392;C01096;C00267;C03267

hsa04978	Mineral absorption	4.85E-05	C00124;C00031;C00041;C00152;C00064;C00407;C00123;C00079;C00148;C00065;C00078;C00183
hsa00970	Aminoacyl-tRNA biosynthesis	8.09E-05	C00041;C00062;C00152;C00097;C00064;C00135;C00407;C00123;C00047;C00079;C00148;C16138;C00065;C00078;C00183;C00101
hsa00140	Steroid hormone biosynthesis	0.00040139	C05488;C05489;C18075;C05284;C05140;C05139;C05499;C05487;C05138;C05290;C05298;C05501;C02373;C00674;C03772;C18045;C04295;C00280;C00523;C11135;C00735;C01227
hsa04742	Taste transduction	0.00111382	C00334;C00020;C11045;C00133;C00095;C00031;C02265;C00740;C00208;C00780;C00089
hsa00270	Cysteine and methionine metabolism	0.00138186	C02356;C00109;C00793;C02218;C00041;C00441;C02291;C00097;C00065;C00409;C01077;C01118;C00022;C00021;C00019;C21015
hsa00260	Glycine, serine and threonine metabolism	0.00222167	C00986;C00109;C00143;C00740;C03283;C00441;C02291;C00097;C00065;C00078;C00546;C00022;C00101
hsa04973	Carbohydrate digestion and absorption	0.00443079	C00246;C00095;C00124;C00031;C00092;C00243;C00208;C00163;C00089
hsa01040	Biosynthesis of unsaturated fatty acids	0.00570773	C08323;C06429;C06428;C06426;C00712;C06427;C16527;C00219;C03242;C08316;C00249;C16525;C06425;C16522;C01530;C08320
hsa04913	Ovarian steroidogenesis	0.00876224	C14770;C05138;C14768;C14769;C04295;C00280;C00219;C01227
hsa00310	Lysine degradation	0.01042917	C01259;C00450;C01149;C01181;C00164;C00487;C04020;C00956;C04076;C00047;C03793;C00042
hsa00500	Starch and sucrose metabolism	0.01042917	C00185;C00095;C00085;C00031;C00103;C00092;C00252;C00208;C00089;C01083

hsa00640	Propanoate metabolism	0.01820643	C00424;C06002;C05984;C00109;C05235;C00546;C02170;C00583;C00163;C00042
hsa04270	Vascular smooth muscle contraction	0.01820643	C14770;C14771;C14748;C14768;C14769;C00219
hsa00250	Alanine, aspartate and glutamate metabolism	0.02095442	C03912;C00334;C00041;C00152;C00064;C03406;C00022;C00042
hsa04726	Serotonergic synapse	0.02363209	C14770;C14771;C14768;C14769;C00219;C00078;C00909;C05956;C00427;C00780
hsa00280	Valine, leucine and isoleucine degradation	0.02363209	C01205;C06001;C06002;C00349;C00164;C03284;C00407;C00123;C00183;C02170
hsa04150	mTOR signaling pathway	0.02571935	C00020;C00062;C00123
hsa00010	Glycolysis / Gluconeogenesis	0.03577246	C06187;C00031;C00103;C00022;C00267;C00668;C00221;C01172
hsa04723	Retrograde endocannabinoid signaling	0.03807027	C13856;C00334;C00219;C00189;C00116;C00427
hsa04922	Glucagon signaling pathway	0.04461446	C00085;C00031;C00103;C00022;C00042;C00668;C01172
hsa00670	One carbon pool by folate	0.04461446	C00445;C00143;C00664;C00101

hsa04931	Insulin resistance	0.04538455	C00095;C00085;C00031;C00092;C02571;C00022

Note: Pathway enrichment analysis was performed using a one-sided hypergeometric test and *p-values* were adjusted for multiple comparisons using the Benjamini-Hochberg (BH) method.

Supplementary Note

Case study 2: Chronic Inflammatory Demyelinating Polyradiculoneuropathy (CIDP) metabolomics study

This case study is based on a previously published metabolomics analysis of metabolic changes in Chronic Inflammatory Demyelinating Polyradiculoneuropathy (CIDP) patients[1]. We retrieved the raw metabolomics data from MetaboLights (ID: MTBLS5828) and processed it using TidyMass2 for peak picking and data cleaning. The original study used conventional approaches to identify and quantify metabolites, perform differential analyses between the CIDP and control groups, and then conduct pathway enrichment separately for positive and negative ion modes. In total, they reported 14 enriched pathways in positive mode and 20 in negative mode using the KEGG database. Because no multiple-testing correction was applied in the original enrichment analysis, we recalculated adjusted *p-values* (n = 200, corresponding to the approximate number of KEGG pathways). Eight pathways reached statistical significance (FDR < 0.05): Bile secretion, Cholesterol metabolism, Purine metabolism, Aldosterone-regulated sodium reabsorption, Steroid hormone biosynthesis, Primary bile acid biosynthesis, Metabolic pathways, and Caffeine metabolism. As "Metabolic pathways" is a very broad category in KEGG, we excluded it, yielding seven final pathways consistent with the original study.

We then applied TidyMass2's metabolic feature-based functional module analysis (FFMA) to the differential features (1,847 total), identifying 15 functional modules with FDR < 0.05 (Supplementary Figure 8a). As expected, most pathways reported by the traditional method mapped to FFMA modules. For example, Steroid hormone biosynthesis is mapped to Module 2 (steroid hormone metabolism), Purine metabolism to Module 4, and Bile secretion to Module 14 (bile acid metabolism) (Supplementary Figure 8b-d).

Notably, FFMA also revealed modules not detected by the traditional approach. For instance, Module 3 corresponds to a core carbohydrate and energy metabolism module encompassing pathways such as Fructose and mannose metabolism, Galactose metabolism, Glucagon signaling, Starch and sucrose metabolism, AMPK signaling, Glycolysis/Gluconeogenesis, and Phenylalanine-Tyrosine-Tryptophan biosynthesis (Supplementary Figure 8e). This module integrates central processes of energy production, redox balance, biosynthetic flux, and energy sensing. Activated immune cells (macrophages, T cells) engaged in demyelination undergo metabolic reprogramming toward glycolysis, the pentose phosphate pathway, and anabolic metabolism to fuel their inflammatory and phagocytic functions[2,3], while Schwann cells rely on intact AMPK signaling for proper myelination and energy homeostasis[4]. Moreover, altered purinergic signaling (ATP/adenosine) and tryptophan-kynurenine metabolism are recognized modulators of neuroimmune cross-talk, and impaired lysosomal clearance of myelin debris can perpetuate inflammation and impede remyelination.

Case study 3: Longitudinal pregnancy plasma metabolomics study

This case study utilizes previously published metabolomics data from a human pregnancy longitudinal study[5]. Raw metabolomics data (Metabolomics Workbench ID: PR000918) were processed using the TidyMass2 framework, encompassing all steps from peak picking to biological interpretation. This analysis identified 1,330 significantly dysregulated metabolic features, with 683 showing an increase and 647 a decrease during pregnancy. The original study mapped 687 annotated compounds to the KEGG database and found that 34 out of 48 pathways showed significant changes (FDR < 0.05). Fifteen out of 34 significant pathways were illustrated in the original paper by the authors, including Steroid hormone biosynthesis, Arachidonic acid metabolism, Amino sugar and nucleotide sugar metabolism, Caffeine metabolism, Ether lipid metabolism, Sphingolipid metabolism, Linoleic acid metabolism, Phenylalanine metabolism, Fatty acid biosynthesis, Retinol metabolism, Tyrosine metabolism, Phenylalanine, tyrosine and tryptophan biosynthesis, Primary bile acid biosynthesis, Nitrogen metabolism, and Aminoacyl-tRNA biosynthesis.

We identified 17 functional modules at FDR < 0.05 with FFMA (Supplementary Figure 9a). Also, most pathways reported by the traditional method mapped to FFMA modules. For example, Aminoacyl-tRNA biosynthesis, Tyrosine metabolism, and Phenylalanine metabolism are mapped to Module 1 (amino acid metabolism). Fatty acid biosynthesis, Linoleic acid metabolism, and Arachidonic acid metabolism to Module 4 (lipid metabolism). Amino sugar and nucleotide sugar metabolism to Module 10, and Steroid hormone biosynthesis to Module 11 (Supplementary Figure 9b-e).

Modules that were not detected by traditional methods were also revealed by FFMA in this case study. For example, Module 2 is associated with carbohydrate transport and utilization and includes pathways such as Galactose metabolism, Fructose and mannose metabolism, ABC transporters, and Carbohydrate digestion and absorption (Supplementary Figure 9f). This module combines dietary sugar processing, intestinal absorption, and systemic transport of monosaccharides, making a positive impact on maternal-fetal energy supply. During pregnancy, maternal glucose homeostasis undergoes marked adaptations, with increased carbohydrate fluxes to support rapid fetal growth and placental function[6]. In particular, Galactose and mannose metabolism are crucial for glycosylation reactions underlying hormone regulation and fetal tissue development[7], while ABC transporters mediate nutrient exchange across placental barriers[8]. And previous research has demonstrated that dysregulation of maternal carbohydrate handling is associated with gestational insulin resistance and gestational diabetes mellitus, conditions that can impair fetal growth trajectories and long-term offspring metabolic health[9,10].

Similarly, Module 12 is another example that was detected by FFMA and represents a module centered on the metabolism of xenobiotics by cytochrome P450 (Supplementary Figure 9g). Cytochrome P450 enzymes mediate the clearance of drugs, dietary compounds, and environmental chemicals[11]. During pregnancy, the hormonal and relevant physiological changes are known to alter CYP450 activity[12,13], thereby influencing maternal drug metabolism, modifying the clearance of xenobiotics, and potentially affecting the extent of fetal exposure. In summary, these examples highlight TidyMass2's ability to uncover novel biological insights beyond existing findings.

Supplementary References

1. Fu, J. *et al.* Metabolic disorder and intestinal microflora dysbiosis in chronic inflammatory demyelinating polyradiculoneuropathy. *Cell Biosci.* **13**, 6 (2023).
2. Pålsson-McDermott, E. M. & O'Neill, L. A. J. Targeting immunometabolism as an anti-inflammatory strategy. *Cell Res.* **30**, 300–314 (2020).
3. Soto-Heredero, G., Gómez de las Heras, M. M., Gabandé-Rodríguez, E., Oller, J. & Mittelbrunn, M. Glycolysis – a key player in the inflammatory response. *FEBS J.* **287**, 3350–3369 (2020).
4. Liu, X. *et al.* AMPK Negatively Regulates Peripheral Myelination via Activation of c-Jun. *Mol. Neurobiol.* **54**, 3554–3564 (2017).
5. Liang, L. *et al.* Metabolic Dynamics and Prediction of Gestational Age and Time to Delivery in Pregnant Women. *Cell* **181**, 1680-1692.e15 (2020).
6. Angueira, A. R. *et al.* New Insights Into Gestational Glucose Metabolism: Lessons Learned From 21st Century Approaches. *Diabetes* **64**, 327–334 (2015).
7. He, M., Zhou, X. & Wang, X. Glycosylation: mechanisms, biological functions and clinical implications. *Signal Transduct. Target. Ther.* **9**, 194 (2024).
8. Joshi, A. A. *et al.* Placental ABC Transporters: Biological Impact and Pharmaceutical Significance. *Pharm. Res.* **33**, 2847–2878 (2016).
9. Murray, S. R. & Reynolds, R. M. Short- and long-term outcomes of gestational diabetes and its treatment on fetal development. *Prenat. Diagn.* **40**, 1085–1091 (2020).
10. Parrettini, S., Caroli, A. & Torlone, E. Nutrition and Metabolic Adaptations in Physiological and Complicated Pregnancy: Focus on Obesity and Gestational Diabetes. *Front. Endocrinol.* **11**, 611929 (2020).
11. Hakkola, J., Hukkanen, J., Turpeinen, M. & Pelkonen, O. Inhibition and induction of CYP enzymes in humans: an update. *Arch. Toxicol.* **94**, 3671–3722 (2020).
12. Isoherranen, N. & Thummel, K. E. Drug Metabolism and Transport During Pregnancy: How Does Drug Disposition Change during Pregnancy and What Are the Mechanisms that Cause Such Changes? *Drug Metab. Dispos.* **41**, 256–262 (2013).
13. Fashe, M. M. *et al.* Impact of pregnancy related hormones on drug metabolizing enzyme and transport protein concentrations in human hepatocytes. *Front. Pharmacol.* **13**, 1004010 (2022).